

Electronic structure of ensembles of gold nanoparticles: Size and proximity effectsHongjian Liu,¹ Bongjin Simon Mun,² Geoff Thornton,³ Steven R. Isaacs,⁴ Young-Seok Shon,⁴ D. Frank Ogletree,¹ and Miquel Salmeron^{1,*}¹*Materials Sciences Division, Lawrence Berkeley National Laboratory, Berkeley, CA 94720, USA*²*Advanced Light Source, Lawrence Berkeley National Laboratory, Berkeley, CA 94720, USA*³*London Centre for Nanotechnology and Chemistry Department, University College London, London WC1H 0AJ, UK*⁴*Department of Chemistry, Western Kentucky University, Bowling Green, KY 42101, USA*

(Received 12 November 2004; revised manuscript received 14 July 2005; published 24 October 2005)

The valence-band electronic structure of alkanethiol stabilized gold nanoparticles (NPs) with different core sizes has been studied using x-ray photoemission spectroscopy. A reduction of density of state near the Fermi level is observed for small particles (<3 nm diam) that are separated by more than 1 nm. A significant cross-coupling between the particles is found when their separation is decreased below 1 nm that restores the density of states at the Fermi edge. The observations are interpreted as a result of changes in the screening of Coulomb blockade effects in the NP system due to tunneling between particles at the shorter separations.

DOI: [10.1103/PhysRevB.72.155430](https://doi.org/10.1103/PhysRevB.72.155430)

PACS number(s): 73.22.-f, 79.60.Jv, 73.23.Hk, 81.07.-b

I. INTRODUCTION

Nanometer metal particles ranging from a few to a few hundred atoms are of interest for science and technology because of their unusual physical and chemical properties, and potential applications in nanoelectronics and bionanoscience. It has been shown that metal nanoparticles (NP) play a particularly important role in electrochemical devices, biological sensing, and catalytic reactions.¹⁻⁵ At the nanometer scale both surface effects and quantum size effects might become important. The first is because of the increasingly large fraction of surface to bulk atoms that could change the electronic structure because of different *d* and *s*-orbital hybridization of surface and bulk atoms. A surface effect could also arise from the binding of adsorbates, for example, ligand molecules often used to stabilize the particles. Quantum effects, on the other hand, give rise to increased spacings of the energy levels and to the formation of energy gaps.^{6,7} The electronic properties can be thus changed from a metallic to semiconductor or even insulator depending on size. These effects have been previously predicted and observed experimentally in the case of semiconductors.^{8,9} DiCenzo *et al.*,¹⁰ using x-ray photoemission spectroscopy (XPS) on mass-selected gold clusters ($Au_n, n=5, 7, 27, 33$) concluded that the small clusters are not metallic and that the transition from metallic to local atomic screening of the core hole occurs at a cluster size of ~ 150 atoms. Later, this size range was narrowed down to $33 < Au_n < 100$.¹¹ With the mass-selected small Au_n^- particles produced by laser vaporization of a pure gold target, photoelectron spectroscopy revealed a significant band gap for Au_{20} of ~ 1.77 eV.¹²

Even if the size of the NP is small enough that the quantum-size effects become measurable using photoelectron spectroscopy, the particles are rarely isolated. In practice, NPs are synthesized by wet chemistry methods and stabilized by organic ligand molecules. The role of the ligand molecules is to make the metal NP chemically inert by bonding to the surface and to prevent them from irreversibly adhering to each other. The electronic structure of NP will then

be influenced by both the quantum-size effect and the surface effects due to the ligands. Boyen *et al.*¹³ demonstrated non-metallic behavior for individual gold clusters of $Au_{55}(PPh_3)_{12}Cl_6$. They concluded that this is due to the effect of chlorine atoms from the $(PPh_3)_{12}Cl_6$ ligand, which actually dominate the electronic properties of the Au_{55} cluster. Recently, Zhang *et al.*¹⁴ presented STM/STS spectroscopic data comparing a ligand molecule and a ligand-stabilized NP and concluded that the energy levels are unlikely introduced by the particular bond between the ligand and the cluster. Discrete energy levels with an average spacing of 170 meV were attributed to the Au_{55} core itself. The effect of the ligands is also manifested in changes in the population of the valence *d* bands and has been shown to give rise to ferromagnetism.^{15,16}

A different but important effect that has been addressed in studies of the electronic structure of NPs is the proximity effects between NPs, and between NPs and the substrate. When the NPs form aggregates and the mutual separations are short, in the nanometer scale, quantum tunneling can become important and can profoundly modify the electronic structure of the ensemble. In this paper we investigate this effect by studying the evolution of the electronic structure in gold NPs as a function of size and mutual separation. The separation is determined by the length of the alkyl chains of the thiol ligands. By changing the chain length we explore the electronic cross-coupling between particles by following the valence-band photoemission intensity, in particular, near the Fermi-level region.

II. EXPERIMENTAL

The gold NPs used in this study have average core diameters of 1.5, 1.7, 3.2, and 4.4 nm and are stabilized by alkanethiol molecules, such as hexanethiol (C6), nonanethiol (C9), dodecanethiol (C12), and pentadecanethiol (C15). The particle core size is determined by the preparation reaction conditions and transmission electron microscopy (TEM).¹⁷

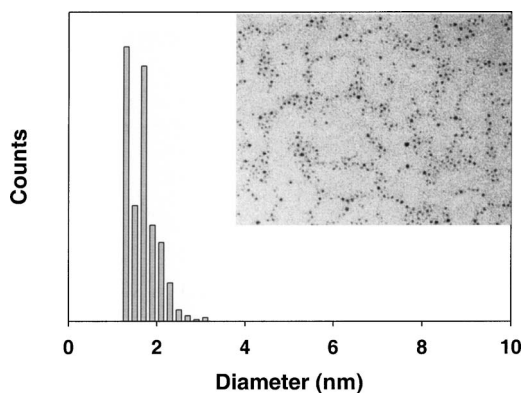


FIG. 1. Histogram showing the size distribution of the 1.7 nm gold nanoparticles stabilized by hexanethiol ligands deposited on an amorphous carbon membrane used for transmission electron microscopy (image shown in inset). The distributions shows an average diameter of 1.7 ± 0.3 nm.

Synthesis was performed following the Brust reaction,^{17,18} where AuCl_4^- is transferred to toluene using tetraoctylammonium bromide as the phase-transfer reagent. Addition of alkanethiols followed by the reduction with NaBH_4 generated alkanethiolate-protected gold NPs. The core size of gold NPs could be controlled by changing the thiol:gold mole ratio and reaction temperature.^{17,19} A histogram and a TEM image of gold NPs with a core size of 1.7 nm is shown in Fig. 1, where the individual NP are well-separated by ligand molecules.

The solvent-suspended gold NPs were deposited onto a silicon wafer substrate covered with a native oxide layer (~ 5 Å) and dried in air to form thin films. This substrate was taped to a metal holder using conductive carbon tape. A small amount of silver epoxy was applied to a corner of the film surface in order to establish good electrical contact between the NP film and the grounded metal support. Because of their short mean-free path, only the photoelectrons originating in the top one or two layers of nanoclusters in the film are measured.

XPS/UPS (ultraviolet photoemission spectroscopy) measurements were carried out at the bending magnet beamline 9.3.2 of the advanced light source. The beamline is equipped with spherical grating monochromator that produces a beam spot size of 0.5×1.0 mm on the sample. The pressure in the chamber was kept below 2×10^{-10} torr during measurements. Spectra were acquired with a SES100 (Scienta) hemispherical electron analyzer with a photon energy of 700 eV for survey spectra and 100 eV photon for energy valence-band spectra. The binding energy scale was calibrated by the position of Au-4*f* core level and the Fermi level of pure gold foil. All spectra were acquired at normal emission and a photon incident angle of 20° from sample surface. The energy resolution was set to 0.3 eV for survey spectra and 0.05 eV for valence-band spectra, respectively. Beam damage was ascertained to be negligible for the duration of the experiments and by repeated measurements at different spots of the sample.

III. RESULTS AND DISCUSSION

Survey XPS spectra were obtained for each sample prior to taking core-level and valence-band spectra to check the

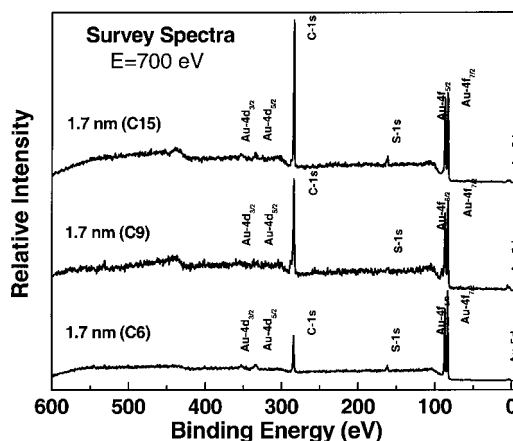


FIG. 2. Survey spectra of gold nanoparticles with 1.7 nm core diameter at an incident photon energy of 700 eV. Spectra for samples separated by alkylthios with chains containing 6, 9, and 12 carbon atoms (C6 to C12) are plotted for comparison. Spectra are normalized to the Au-4*f*_{7/2} peak intensity. The broad peak near 430 eV is the Auger peak of carbon.

sample quality. Typical spectra for 1.7 nm particles with different ligand lengths are shown in Fig. 2. All spectra are normalized to the Au-4*f*_{7/2} peak intensity. The spectra contain the expected photoelectron peaks from the materials in the sample, i.e., Au-5*d* valence band, Au-4*f* and Au-4*d* core level from Au NP, and the C-1*s* and S-1*s* from the ligand molecules. The relative intensity of the C-1*s* peak varies as expected with the length of the alkyl chains of the ligand.

The valence band was measured in two different settings, a long region to cover the entire valence band, from -5 to 25 eV binding energy, and short, higher resolution region around the Fermi edge, from -2.5 to 3.5 eV. The results are shown in Figs. 3 and 4, respectively. The spectra in Fig. 4 are normalized to the intensity of the 5*d*_{5/2} peak in long scan spectra, where there is no overlap with the C-derived bands.

Comparing to the spectrum of the pure gold foil in Fig. 3, it can be seen that the photoemission features in the NP are

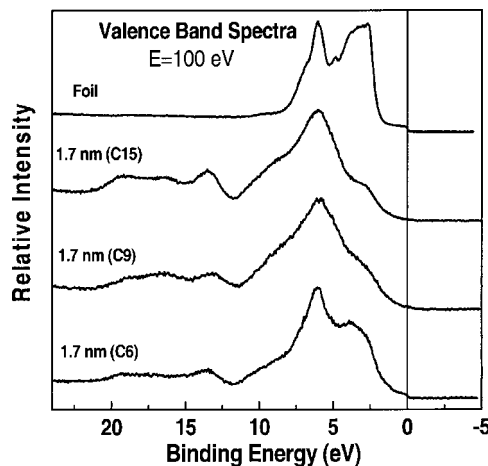


FIG. 3. Valence-band spectra of gold nanoparticles with 1.7 nm core diameter at an incident photon energy of 100 eV. A gold foil spectrum is shown as comparison.

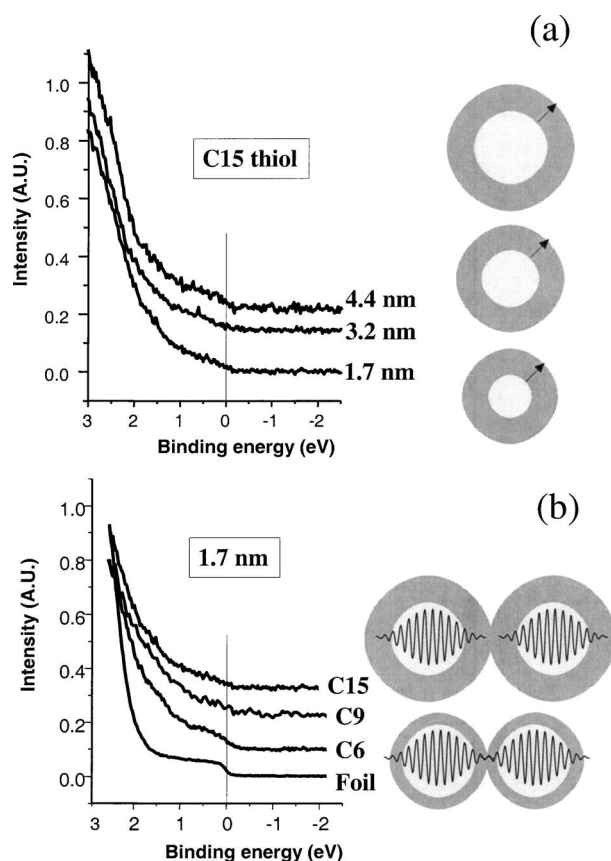


FIG. 4. Expanded view of the density of states of gold nanoparticles near the Fermi level. The incident photon energy is 100 eV. Each spectrum is normalized to the intensity of its $5d_{5/2}$ peak (see Fig. 3). (a) Particles of 1.7, 3.2, and 4.4 nm core diameter with a large separation (a C15 ligand); (b) the effect of interparticle separation (as determined by the length of the alkyl chains in the ligand) is clearly visible in these curves, corresponding to particles with 1.7 nm core diameter. Short separations (<1 nm) restore the density of states observed for larger particles.

changed from those of the bulk metal. The spectrum consists of two regions. The region in the 0–5 eV binding-energy range is mainly contributed by Au- $5d_{5/2}$ and $6s$ derived states. The peak at ~ 7.0 eV is due to Au- $5d_{3/2}$ levels plus a substantial contribution from the C- $2p$ emission from the ligand molecules. This causes the intensity ratio between the 3.5 and 6.0 eV peaks to decrease with increasing ligand chain length. The other region with binding energy between 12 and 22 eV is due to the C- $2s$ levels of the ligand molecules. There are two peaks with a 5.6 eV interval. The stronger peak at ~ 13.8 eV was suggested as fingerprint of a zigzag planar conformation of the alkanethiol molecule.²⁰ The C- $2s$ features are clearly more pronounced for the particles with long ligand chain.

A key issue in our study is the extent of the spectral contribution from the ligand molecules to the density of states, especially near the Fermi-level region. Our valence-band spectra were excited by 100 eV photons. At this energy the photoionization cross section for Au- $5d$ is about five times that of the C- $2s$ and ten times of that of the C- $2p$ levels.²¹ Thus the contribution from the Au levels should be dominant

over those from the C- $2s$ and C- $2p$ levels of the alkanethiol ligand molecules in the valence-band. By comparing the valence-band spectra of alkanethiol monolayers prepared on a gold substrate and pure gold, using synchrotron radiation and HeI light, Duwez *et al.*²⁰ showed that the Au- $5d$ contribution is dominant in the low binding-energy side of the valence band, i.e., the region from Fermi-level position to ~ 3.5 eV. Their UPS spectra of alkanethiols showed that there is a flat background in this region, from the Fermi-level position to about 3.5 eV, indicating that indeed the contribution of alkanethiols (C- $2p$) to the density of states near Fermi level is negligible. Therefore, it can be safely assumed that the spectrum of the gold NPs in the binding-energy region from 0 to 3.5 eV reflects only the contribution from the Au levels of the NPs.

The region of the valence-band spectra near the Fermi edge shown in Fig. 4(a) shows a substantial loss of emission at the Fermi edge when the particle size decreases below 4 nm for ligands with alkyl chains of 9, 12, and 15 carbon atoms. Since the results for all these chain lengths were similar only the 15 carbon chain results are shown. Interestingly however, when the length of the ligand chain decreased from 9 to 6 carbon units, the intensity of the Fermi edge emission of small particles (1.5 and 1.7 nm) recovered to a value similar to that of the large particles. This is shown in Fig. 4(b) where the Fermi edge emission of the 1.7 nm particles with ligands of different length is compared.

Since the effect of the ligands is to separate the metallic cores to a distance of the order of twice their chain length, we consider the following effects to explain the observed changes in electronic structure: (i) electronic quantum confinement; (ii) increased fraction of surface atoms; and (iii) Coulomb blockade or capacitance effects.

Quantum confinement is related to the uncertainty principle, which states that as the spatial range available to the electrons decreases there should be an increase in their kinetic energy (which is manifested in an increased separation between the energy levels). This effect should be felt most strongly by the more delocalized electron states derived from the $6s$ Au atomic orbitals, which form the Fermi edge. For particle diameters of 1.5 and 1.7 nm, electron confinement should increase the energy separation of such states by approximately 0.025–0.037 eV, based on the free-electron model.⁶ Such values are comparable to the thermal energy at room temperature ($kT \sim 0.025$ eV) and, therefore, should be undetectable in our experiments.

The second effect is the increasing fraction of Au atoms present at the surface, which are less coordinated than in the bulk and/or bound to S atoms of the thiol ligands. According to the magic-number rule, the number of atoms in the n th shell is $(10n^2+2)$.⁷ This gives 92 surface atoms for a 147-atom particle (~ 1.5 nm) or about 63% of the total. The next closed-shell particle, of 2.3 nm diam, contains 309 atoms, with surface atoms comprising 52% of the total. The emission from these surface atoms is also enhanced relative to bulk atoms due to attenuation of the emitted photoelectrons from deeper inside the particle. The lower-coordination Au surface atoms and the Au atoms bound to S should therefore dominate the photoemission spectrum in small particles (<3 nm diameter). The S—Au bonds remove mostly s but

also some *d*-band electrons into localized bonding orbitals.^{22,23} The loss of *d*-orbital electrons could give rise to a magnetic moment in the NP; a result that has been recently observed.^{15,16} Because each S atom nominally binds one electron and the ratio of thiol molecules to Au surface atoms is roughly 1:3 (assuming a S density as in the $\sqrt{3} \times \sqrt{3}$ adlayer structure that forms on the (111) face), the number of *s* electrons formally removed by formation of S—Au bonds should be about 30%, leaving still “free” or metallic electrons to contribute to Fermi-level emission. Since the observed loss of intensity at the Fermi level is larger than this number, we conclude that other effects must be playing a role.

We propose these to be Coulomb blockade effects, which also explain the strong influence of interparticle separation, shown in Fig. 4(b). Small metal clusters, unlike bulk metal, are characterized by a size-dependent finite capacitance, $C(r) = 4\pi\epsilon_0\epsilon r$, where r is the radius of the particle, ϵ_0 is the permittivity of vacuum, and ϵ is the dielectric constant of the organic material surrounding the particle.^{24,25} The energy needed to charge (add or remove) an electron in an individual particle is given by $U_c = e^2/2C$. For our 1.5–1.7 nm particle surrounded by alkanethiol groups, choosing $\epsilon = 2.2$,²⁶ U_c is about 0.5 eV, i.e., ten times bigger than kT at room temperature. The effect of the blockade would be a shift of the *s* band down in the binding energy scale of that amount, which would explain the observed loss of intensity.

When the interparticle separation distance becomes < 1 nm, quantum tunneling of electrons across the particles becomes important and provides the screening that eliminates the charging energy at the local level. It has been indeed observed that in small cluster systems, exchange interactions and electronic delocalization become significant at interparticle separation $d \leq 0.5$ nm.⁸ Studies of a Langmuir monolayer formed by ligand-capped silver NPs of 2.6–3.5 nm diam, showed that the coupling between particles increases with decreasing distance between nearest-particle centers.^{27–29} For $1.3 > D/2R > 1.2$ (D =distance between nearest particle centers, R =particle radius), these authors found that quantum coupling dominates the electronic properties of the monolayer. When $D/2R \sim 1.2$, they propose that exchange interactions give rise to the insulator-

to-metal transition and the Coulomb band gap disappear.²⁹ When our gold NPs of 1.5 and 1.7 nm are capped with hexanethiol (C6) ligands, their separation is small enough for tunneling to occur with sufficient probability and to produce a substantial increase of density of states at the Fermi level. It is known that the separation provided by the alkyl chains can be substantially less than twice their length because of the overlapping of chains from nearest particles upon the formation of NP film.⁸ Previous results from a monolayer silver NP showed that hexanethiol (C6) and pentanethiol (C5) caps maintain $\sim 0.5 \pm 0.2$ nm separation, whereas decanethiol (C10) caps maintain $\sim 1.1 \pm 0.2$ nm separation.²⁹

IV. CONCLUSIONS

We have used photoelectron spectroscopy to investigate the effect of size and separation on the electronic properties of ligand-stabilized gold nanoparticles. We have found a reduction of the density of states at the Fermi level when the particle size becomes < 3 nm and the particles are separated by ligands with alkane chains of more than nine carbon units. We have observed an increase of the density of states when the small gold particles are brought closer, which we accomplished by using shorter ligand chains of six carbon units. We propose that the reduction in density of states can best be explained by Coulomb blockade effects when the particle separation is > 1 nm. The recovery of the density of states when the particle separation decreased can be explained as a result of electronic cross-coupling due to electron tunneling. This effect plays a crucial role in determining the character (metallic or insulating) of the film. Films made of nanoparticles separated by < 1 nm behave effectively as a collective metal, even though each particle, if isolated, would have a nonmetallic character.

ACKNOWLEDGMENTS

This work was supported by the Director, Office of Energy Research, Office of Basic Energy Sciences, Division of Chemical Sciences, Geosciences, and Biosciences, of the U.S. Department of Energy under Contract No. DE-AC03-76SF00098. G.T. thanks EPSRC (UK) for support.

*Email address: mbsalmeron@lbl.gov

¹Y. W. C. Cao, R. C. Jin, and C. A. Mirkin, *Science* **297**, 1536 (2002).

²P. V. Kamat, *J. Phys. Chem. B* **106**, 7729 (2002).

³M. Valden, X. Lai, and D. W. Goodman, *Science* **281**, 1647 (1998).

⁴P. C. Biswas, Y. Nodasaka, and M. Haruta, *J. Electroanal. Chem.* **381**, 167 (1995).

⁵Y. Xiao, F. Patolsky, E. Katz, J. F. Hainfeld, and I. Willner, *Science* **299**, 1877 (2003).

⁶W. P. Halperin, *Rev. Mod. Phys.* **58**, 533 (1986).

⁷G. Schmid, *Chem. Rev. (Washington, D.C.)* **92**, 1709 (1992).

⁸C. B. Murray, C. R. Kagan, and M. G. Bawendi, *Annu. Rev.*

Mater. Sci. **30**, 545 (2000).

⁹M. Behboudnia and P. Sen, *Phys. Rev. B* **63**, 035316 (2001).

¹⁰S. B. DiCenzo, S. D. Berry, and E. H. Hartford, Jr., *Phys. Rev. B* **38**, 8465 (1988).

¹¹H.-G. Boyen, Th. Herzog, G. Kastle, F. Weigl, P. Ziemann, J. P. Spatz, M. Moller, R. Wahrenberg, M. G. Garnier, and P. Oelhafen, *Phys. Rev. B* **65**, 075412 (2002).

¹²J. Li, X. Li, H. J. Zhai, and L. S. Wang, *Science* **299**, 864 (2003).

¹³H.-G. Boyen, G. Kastle, F. Weigl, P. Ziemann, G. Schmid, M. G. Garnier, and P. Oelhafen, *Phys. Rev. Lett.* **87**, 276401 (2001).

¹⁴H. J. Zhang, G. Schmid, and U. Hartmann, *Nano Lett.* **3**, 305 (2003).

¹⁵P. Crespo, R. Litran, T. C. Rojas, M. Multigner, J. M. de la Fu-

- ente, J. C. Sanchez-Lopez, M. A. Garcia, A. Hernando, S. Penades, and A. Fernandez, *Phys. Rev. Lett.* **93**, 087204 (2004).
- ¹⁶Y. Yamamoto, T. Miura, T. Teranishi, M. Miyake, H. Hori, M. Suzuki, N. Kawamura, H. Miyagawa, T. Nakamura, and K. Kobayashi, *Phys. Rev. Lett.* **93**, 116801 (2004).
- ¹⁷M. J. Hostetler, J. Wingate, C.-J. Zhong, J. E. Harris, R. W. Vachet, M. R. Clark, J. D. Londono, S. J. Green, J. J. Stokes, G. D. Wignall, G. L. Glish, M. D. Porter, N. D. Evans, and R. W. Murray, *Langmuir* **14**, 17 (1998).
- ¹⁸M. Brust, M. Walker, D. Bethell, D. J. Schiffrin, and R. Whyman, *J. Chem. Soc., Chem. Commun.* , 801 (1994).
- ¹⁹J. T. Hicks, D. T. Miles, and R. W. Murray, *J. Am. Chem. Soc.* **124**, 13322 (2002).
- ²⁰A.-S. Duwez, S. Di Paolo, J. Ghijsen, J. Riga, M. Deleuze, and J. Delhalle, *J. Phys. Chem. B* **101**, 884 (1997).
- ²¹J. J. Yeh and I. Lindau, *At. Data Nucl. Data Tables* **32**, 1 (1985).
- ²²P. Zhang and T. K. Sham, *Appl. Phys. Lett.* **81**, 736 (2002).
- ²³P. Zhang and T. K. Sham, *Phys. Rev. Lett.* **90**, 245502 (2003).
- ²⁴I. S. Weitz, J. L. Sample, R. Ries, E. M. Spain, and J. R. Heath, *J. Phys. Chem. B* **104**, 4288 (2000).
- ²⁵G. Markovich, C. P. Collier, S. E. Henrichs, F. Remacle, R. D. Levine, and J. R. Heath, *Acc. Chem. Res.* **32**, 415 (1999).
- ²⁶K. Slowinski, R. V. Chamberlain, R. Bilewicz, and M. Majada, *J. Am. Chem. Soc.* **118**, 4709 (1996).
- ²⁷C. P. Collier, R. J. Saykally, J. J. Shiang, S. E. Henrichs, and J. R. Heath, *Science* **277**, 1978 (1977).
- ²⁸G. Markovich, C. P. Collier, and J. R. Heath, *Phys. Rev. Lett.* **80**, 3807 (1998).
- ²⁹G. Medeiros-Ribeiro, D. A. A. Ohlberg, R. S. Williams, and J. R. Heath, *Phys. Rev. B* **59**, 1633 (1999).